

## A multi-machine analysis of non-axisymmetric and rotating halo currents

C. E. Myers<sup>1</sup>, S. P. Gerhardt<sup>1</sup>, N. W. Eidietis<sup>2</sup>, R. S. Granetz<sup>3</sup>, G. Pautasso<sup>4</sup>, and the ITPA Working Group on Non-Axisymmetric Halo Currents.

email: Clayton Myers, [cmyers@pppl.gov](mailto:cmyers@pppl.gov)

<sup>1</sup> Princeton Plasma Physics Laboratory

<sup>2</sup> General Atomics, San Diego, CA, USA

<sup>3</sup> Massachusetts Institute of Technology

<sup>4</sup> Max-Planck IPP, Garching, Germany

Large halo currents are often driven in the metal components of a tokamak vessel when a disrupting plasma comes into contact with the plasma facing components. Halo currents are known to exhibit non-axisymmetric and rotating features in several machines including Alcator C-Mod [1], DIII-D [2], ASDEX Upgrade [3], and NSTX [4]. Such non-axisymmetries are of great interest to ITER because they can increase mechanical stresses during a disruption, especially if the rotation resonates with the natural frequencies of the vessel [5]. This paper presents an ITPA-initiated multi-machine analysis of these phenomena. The ITPA non-axisymmetric halo current database presently includes data from C-Mod, DIII-D, AUG, and NSTX. These data are processed within a common analytical framework to facilitate direct comparisons between devices.

Figure 1 shows representative halo current measurements from each of the four devices in the ITPA non-axisymmetric halo current database. These data are obtained from toroidally resolved arrays of halo current sensors that are comprised of either shunt tiles or segmented rogowski coils. In each panel of the figure, the halo current amplitude,  $I_h$ , is plotted in color as a function of time and toroidal angle. Time is normalized to the characteristic ‘fast’ quench timescale for each device,  $\tau_{CQ}$ . The black lines represent the toroidal phase of the rotating halo current lobe. It is clear that significant non-axisymmetries and rotation are observed in each device. Furthermore, similar rotation frequencies are observed across devices. In light of the current-quench-normalized timebase, this indicates that the physics driving the halo current rotation may be linked to the physics of the current quench.

The details of the analysis presented in Fig. 1 are shown in Fig. 2. In order to quantify the non-axisymmetry and rotation, the data are toroidally decomposed at each time point using a simplified model function of the form  $I_h(\phi) = h_0 + h_1 \sin(\phi - h_2)$ , where  $\phi$  is the toroidal angle,  $h_0$  is the  $n=0$  amplitude,  $h_1$  is the  $n=1$  amplitude, and  $h_2$  is the  $n=1$  phase. In Fig. 2,  $h_0$  and  $h_1$  have comparable amplitudes until late in the disruption when  $h_1$  decays away and the halo currents symmetrize. This late symmetrization, which is frequently observed, is likely due to the loss of closed magnetic surfaces in the plasma. Finally, in order to quantify the total amount of rotation during a given halo current pulse,  $h_2/2\pi$  is integrated in time. More than two complete rotations are observed during the sample DIII-D disruption shown in Fig. 2.

The results from the halo current analysis in Fig. 2 facilitate the correlation of various quantities of interest across the ITPA non-axisymmetric halo current database. In Fig. 3a, total rotation is plotted against measured non-axisymmetry. Here, non-axisymmetry is quantified in terms of the toroidal peaking factor,  $TPF = \max\{I_h(\phi)\}/\text{mean}\{I_h(\phi)\}$ , while rotation is quantified using the total rotations metric from

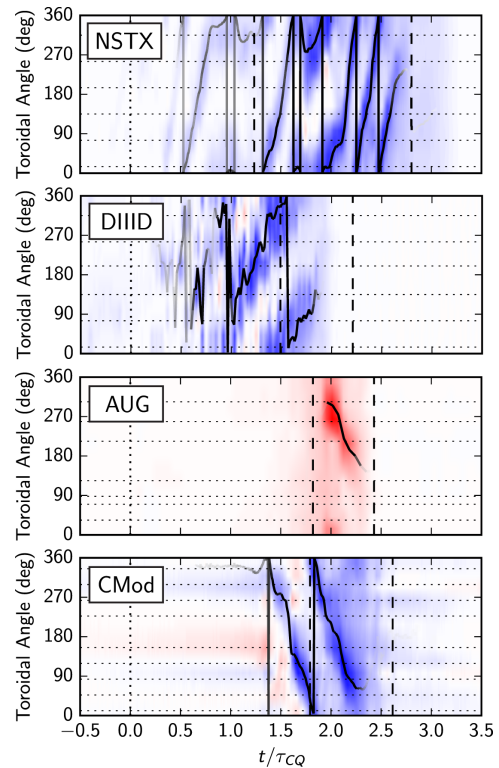


Fig. 1: Toroidally resolved measurements of non-axisymmetric and rotating halo currents in four different devices. Color represents the halo current magnitude, while the black lines track the toroidal phase of the rotating halo current lobe. Time is normalized to the characteristic fast quench time for each device,  $\tau_{CQ}$ .

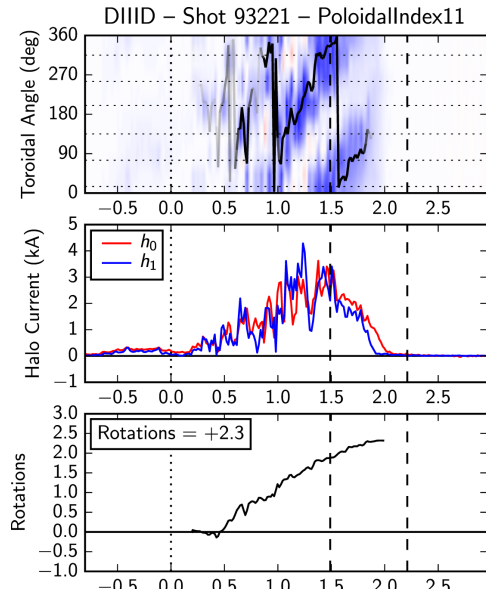


Fig. 2: Sample analysis of DIII-D halo currents. The  $n=0$  and  $n=1$  mode amplitudes ( $h_0$  and  $h_1$ ) are comparable in magnitude until the halo currents symmetrize late in the disruption. More than two complete rotations are observed.

Fig. 2. It is clear from Fig. 3a that non-axisymmetry and rotation are positively correlated, and that NSTX shows the most rotation among the four machines in the database. C-Mod and DIII-D, on the other hand, produce two types of halo currents. Each has a cluster of quasi-symmetric halo currents at low TPF and low rotation that contrast with a second set of halo currents that exhibit strong non-axisymmetry, many of which exceed one complete rotation in the vessel.

Finally, in Fig. 3b, the measured non-axisymmetry (TPF) is plotted against the halo current magnitude. Here, the ‘halo current magnitude’ is defined as the temporal maximum of the toroidal RMS of  $I_h(\phi)$ . It is normalized to the 90<sup>th</sup> percentile of all halo current magnitudes for a given device rather than to the conventional pre-disruption plasma current. As Fig. 3b shows, this halo current magnitude and the toroidal peaking factor are *positively correlated*. This correlation runs counter to the published trend between the TPF and the ‘halo current fraction,’ which is instead defined as the total inferred halo current normalized to the pre-disruption plasma current [see Fig. 6 in Ref. 6]. These results highlight the importance of determining the relationship between the halo current magnitude and the halo current fraction. If it is in fact the case that larger halo current magnitudes produce larger non-axisymmetries, then it is even more imperative for the success of ITER to understand the physical processes that drive halo current non-axisymmetries and rotation.

axisymmetries, then it is even more imperative for the success of ITER to understand the physical processes that drive halo current non-axisymmetries and rotation.

This work was supported by U.S. DOE Contract D-AC02-09CH11466

- [1] R. S. Granetz et al., *Nucl. Fusion* **36**, 545 (1996)
- [2] T. Evans et al., *J. Nucl. Mat.* **241-243**, 606 (1997)
- [3] G. Pautasso, et al., *Nucl. Fusion* **51**, 043010 (2011)
- [4] S. P. Gerhardt, *Nucl. Fusion* **53**, 023005 (2013)
- [5] T. Hender et al., *Nucl. Fusion* **47**, S128 (2007)
- [6] N. W. Eidietis et al., *Nucl. Fusion* **55**, 063030 (2015)

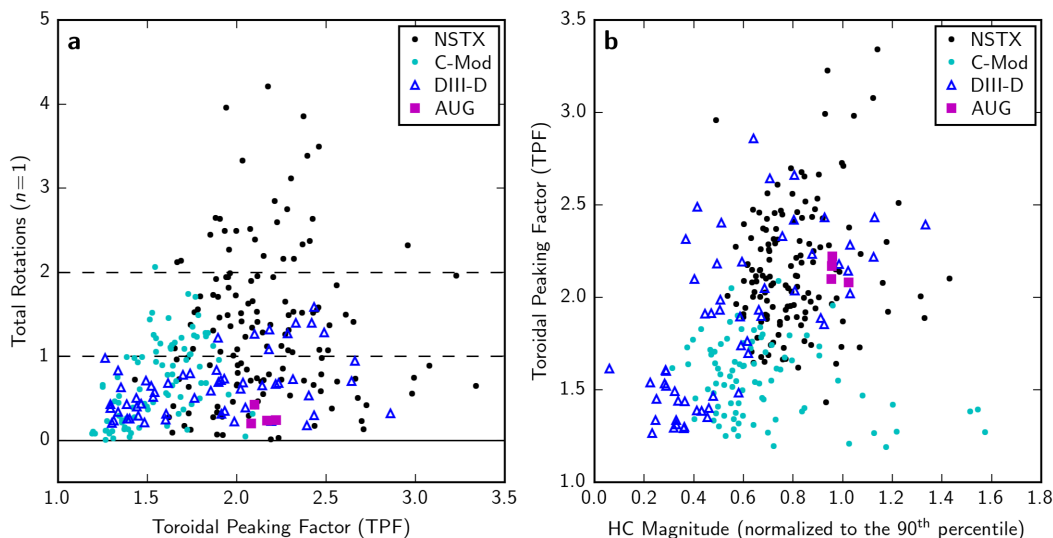


Fig. 3: Scatterplots of non-axisymmetry (toroidal peaking factor), rotation, and halo current magnitude from the ITPA non-axisymmetric halo current database. The halo current magnitude is normalized to the 90<sup>th</sup> percentile of halo current magnitudes from each device.